

ARTICLE

Chemical Vapor Deposition Mechanism of Copper Films on Silicon Substrates

Song Wu, Bo Tao, Yong-ping Shen, Qi Wang*

Department of Chemistry, Zhejiang University, Hangzhou 310027, China

(Dated: Received on June 8, 2005; Accepted on December 5, 2005)

A versatile metal-organic chemical vapor deposition (MOCVD) system was designed and constructed. Copper films were deposited on silicon (100) substrates by chemical vapor deposition (CVD) using $\text{Cu}(\text{hfac})_2$ as a precursor. The growth of Cu nucleus on silicon substrates by H_2 reduction of $\text{Cu}(\text{hfac})_2$ was studied by atomic force microscopy and scanning electron microscopy. The growth mode of Cu nucleus is initially Volmer-Weber mode (island), and then transforms to Stranski-Rastanov mode (layer-by-layer plus island). The mechanism of Cu nucleation on silicon (100) substrates was further investigated by X-ray photoelectron spectroscopy. From Cu2p, O1s, F1s, Si2p patterns, the observed C=O, OH and CF_3/CF_2 should belong to $\text{Cu}(\text{hfac})$ formed by the thermal dissociation of $\text{Cu}(\text{hfac})_2$. H_2 reacts with hfac on the surface, producing OH. With its accumulation, OH reacts with hfac, forming HO-hfac, and desorbs, meanwhile, the copper oxide is reduced, and thus the redox reaction between $\text{Cu}(\text{hfac})_2$ and H_2 occurs.

Key words: Metal-organic chemical vapor deposition, Copper film, Silicon (100), Deposition reaction mechanism

I. INTRODUCTION

In the process of ultra large-scale integrated circuits (ULSI) fabrication, metallization is a significant procedure, which refers to the metal layers that electrically interconnect the various structured devices fabricated on the silicon substrate [1]. Aluminum and aluminum alloys have been the choice for interconnection metals. However, they have a high interconnect delay (RC time delay) and serious electromigration (EM), which limits their performance and reliability in ULSI. Compared with the aluminum alloys, copper has lower resistivity and higher resistance to EM and stressmigration (SM). To fabricate the high-performance interconnects with low RC delay, the integration of low resistivity metal wiring and low-k intermetal dielectric is crucial for next-generation ULSI technology [2-4].

Due to its low resistivity [5,6] and high electromigration resistance [7], copper is widely predicted to be the interconnect material replacing aluminum and aluminum alloys for technologies below $0.25 \mu\text{m}$. Copper (Cu) films [8] are the best metallization candidate to replace aluminum and aluminum alloys. To implement copper into a metal line via interconnects, the dual damascene process is required because copper is difficult to be etched. Among various methods to deposit copper, metallorganic chemical vapor deposition (MOCVD) processes have several advantages such as the ability to achieve the high aspect ratio and the good

step coverage [9]. Thus, it is of significance to study the growth of Cu films, of the Cu nucleus, and the mechanism of chemical vapor deposited Cu films on silicon substrates.

II. EXPERIMENTAL

The MOCVD apparatus (shown in Fig.1) used in this work consists of three sub-systems: precursor supplying system, reaction system and high vacuum system. The precursor supplying system consists of carrier gas mass flow controller (MFC) and precursor evaporator. The CVD reaction system is mainly a reactor, which contains a high vacuum obturating chamber, a knock-down sample holder and four well-controlled heaters. The high vacuum system is composed of a mechanical pump, a turbo pump, and a cold trap, which is designed for preventing pump from polluting.

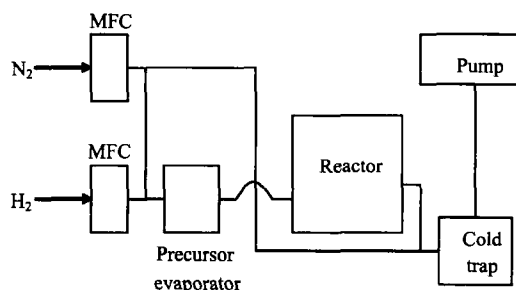


FIG. 1 Scheme of MOCVD apparatus.

The thin copper films were grown in a vertical, cold wall (80°C) reactor. The precursor, $\text{Cu}(\text{hfac})_2 \cdot n\text{H}_2\text{O}$

* Author to whom correspondence should be addressed. E-mail: qiwang@zju.edu.cn; Tel: 0571-87952424; Fax: 0571-87951895.

(Copper(II) hexafluoroacetylacetonate hydrate) was evaporated at 80 °C. The substrate was cut from a Si(100) wafer (n type). The initial reaction temperature was set to be 350 °C. Firstly, the deposition pressure and the substrate direction were optimized, then, the deposition temperature, and finally the deposition time was optimized. And other experimental conditions were also adjusted according to the references [10, 11]. XRD and SEM results show that the optimized conditions are as following: Si substrates cleaned by 2% HF solution firstly, background pressure 133 μ Pa, deposition temperature 350 °C, deposition pressure 400 Pa, flow rate of carrier gas H₂ 20 sccm (standard cubic centimeter), and deposition time 7 min, which form preferable morphology and crystallization. The (111) texture can be observed on thin Cu film deposited under the optimized conditions. Figure 2 shows the SEM morphology under the optimized conditions, indicating that the silicon substrate is covered with dense copper films. As previously reported by Mukhopadhyay [12], when Cu(tbob)₂ (copper *t*-butylacetoacetate) was used as precursor to deposit copper on SiO₂/Si(100) substrate, it was observed that the amount of deposited carbon (a kind of impurity) decreased with increasing temperature and decreasing pressure. Carbon-free pure copper was obtained at 400 °C and above, when the total reactor pressure is 1330 Pa and below. Therefore, it should be expected that there is almost no carbon deposited on the substrate surface at reaction temperature 350 °C and at lower pressure of 400 Pa in this work.

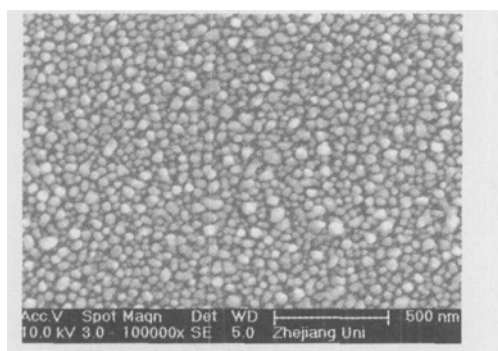


FIG. 2 SEM micrograph of Cu film at the optimized deposition conditions.

III. RESULTS AND DISCUSSION

A. The Cu nucleation on substrate

Atomic force microscopy (AFM) has been extensively used to study the growth mechanism of thin films [13]. The AFM micrographs of Cu films on Si substrate at different deposition times (3, 5, 7 min) are shown in Fig.3, and the related AFM grain analysis is presented in Table I.

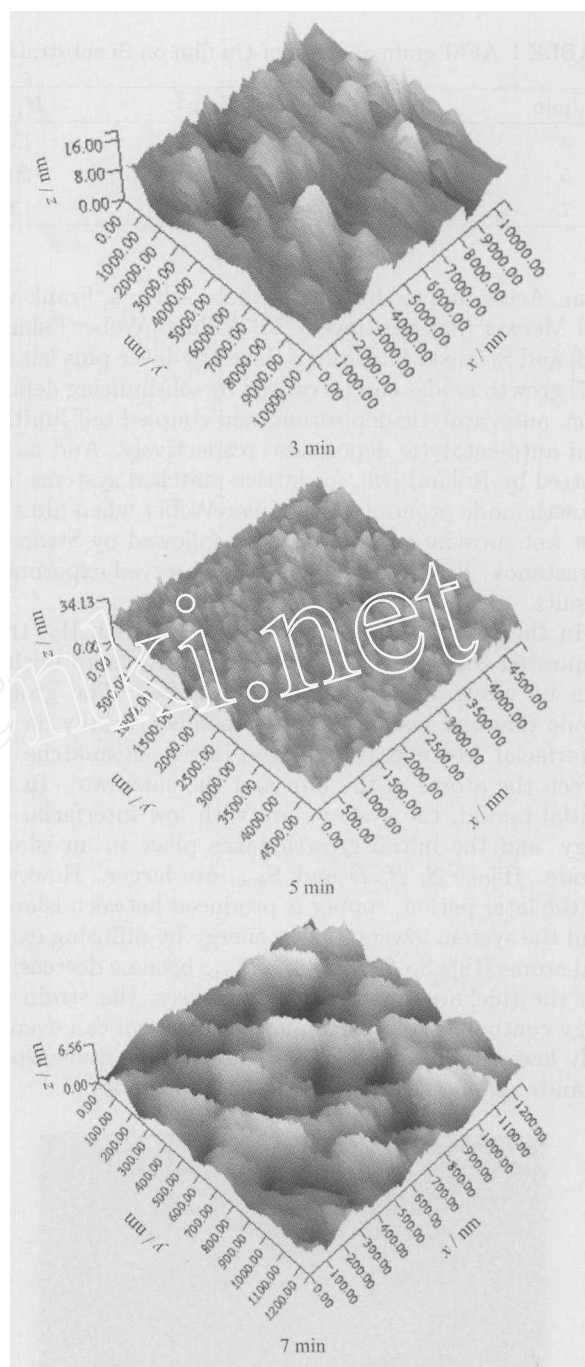


FIG. 3 AFM micrographs of Cu film on Si substrate at different deposition times.

From AFM analysis, it can be found that the average area (S), the average height (H), the average diameter (D), the maximum area (S_{\max}) and the minimum area (S_{\min}) decrease with increasing deposition time, which means that the Cu films are more uniform and compact. As previously observed by Puurunen [14], there are generally three types of sticking processes: self-limiting, random, and auto-catalytic deposi-

TABLE I AFM grain analysis of Cu film on Si substrate at different deposition times

t /min	N	S/nm^2	H/nm	D/nm	$S_{\text{max}}/\text{nm}^2$	$S_{\text{min}}/\text{nm}^2$
3	281	605371	11.83	438.97	3780274	26917
5	275	31191	20.18	99.64	136035	707
7	315	599	3.41	13.80	3940	41

tion. According to this classification schema, Frank-van der Merwer (layer-by-layer) [15], Volmer-Weber (island) [16] and Stranski-Krastanov (layer-by-layer plus island) [17] growth modes can be caused by self-limiting deposition, autocatalytic deposition, and coupled self-limiting and auto-catalytic deposition, respectively. And as reported by Roland [18], for lattice-matched systems, the growth mode prone to be Volmer-Weber when films do not wet substrates, which is then followed by Stranski-Krastanov. It agrees well with the observed experiment results.

In the reactor, the precursor reacted with H_2 , then deposited copper seeds at the positions where nucleus can be easily formed on the substrate. The growth mode that the system adopts depends crucially on the interfacial free energy, and the lattice mismatches between the atoms in the film and the substrate. In the initial period, the systems are with low interfacial energy, and the initial growth takes place in an island-mode. Hence S , H , D and S_{max} are larger. However, in the later period, copper is produced between islands, and the system lowers its free energy by diffusing external atoms [19]. So S , H , D and S_{max} become decreasing. As the thickness furthermore increases, the strain energy continues to build up, and the system can eventually lower its free energy by forming three-dimensional islands again, as shown in Fig.4 (white spots).

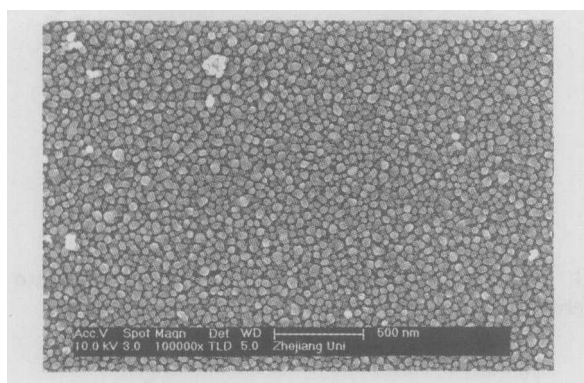


FIG. 4 SEM micrograph of Cu film on Si substrate, 7 min.

B. The reaction mechanism of Cu deposition

X-ray photoelectron spectroscopy (XPS) can be used to characterize the surface components [20,21], thus it

was usually used to investigate reaction mechanism. The XPS patterns (CAE mode, 50 eV, anodes of Mg $K\alpha$ with radiation at 1253.6 eV) of Cu film on Si substrate at different deposition times (3,5,7 min) are shown in Fig.5, and the peak fitting results are presented in Table II.

TABLE II The results of XPS data analysis (peak fitting)

Elements	t /min	Position*/eV	FWHM/eV	Area	
Cu2p	3	933.09	2.29	85220	
		944.16	2.75	9530	
		952.95	2.87	47498	
	5	932.84	2.07	178406	
		944.19	3.01	23661	
		952.73	2.39	102868	
		943.97	3.02	38602	
	7	932.79	1.85	266682	
		943.97	3.02	38602	
		952.68	2.38	145006	
	Si2p	3	99.18	1.33	21719
			102.75	2.50	9225
5		99.19	1.36	13804	
		102.66	1.63	4599	
7		99.13	1.36	6186	
		102.24	2.82	2718	
O1s	3	530.01	1.50	4167	
		532.27	2.40	84815	
	5	530.40	1.61	10284	
		532.26	2.55	68140	
	7	530.24	1.17	4159	
		531.58	3.05	64092	
		532.25	1.00	264	
	F1s	3	687.44	3.65	12861
			687.47	3.14	15559
5		688.16	1.42	2802	
		687.81	2.63	22499	

* Calibrated by C1s 284.8 eV.

The high-resolution peaks are fitted using the XPS-PEAK program, version 4.1 (Raimund W. Kwok, University of Hong Kong). A Shirley background subtraction is applied and Gauss-Lorentz Sum curves are used for the curve fitting. According to the database PHI

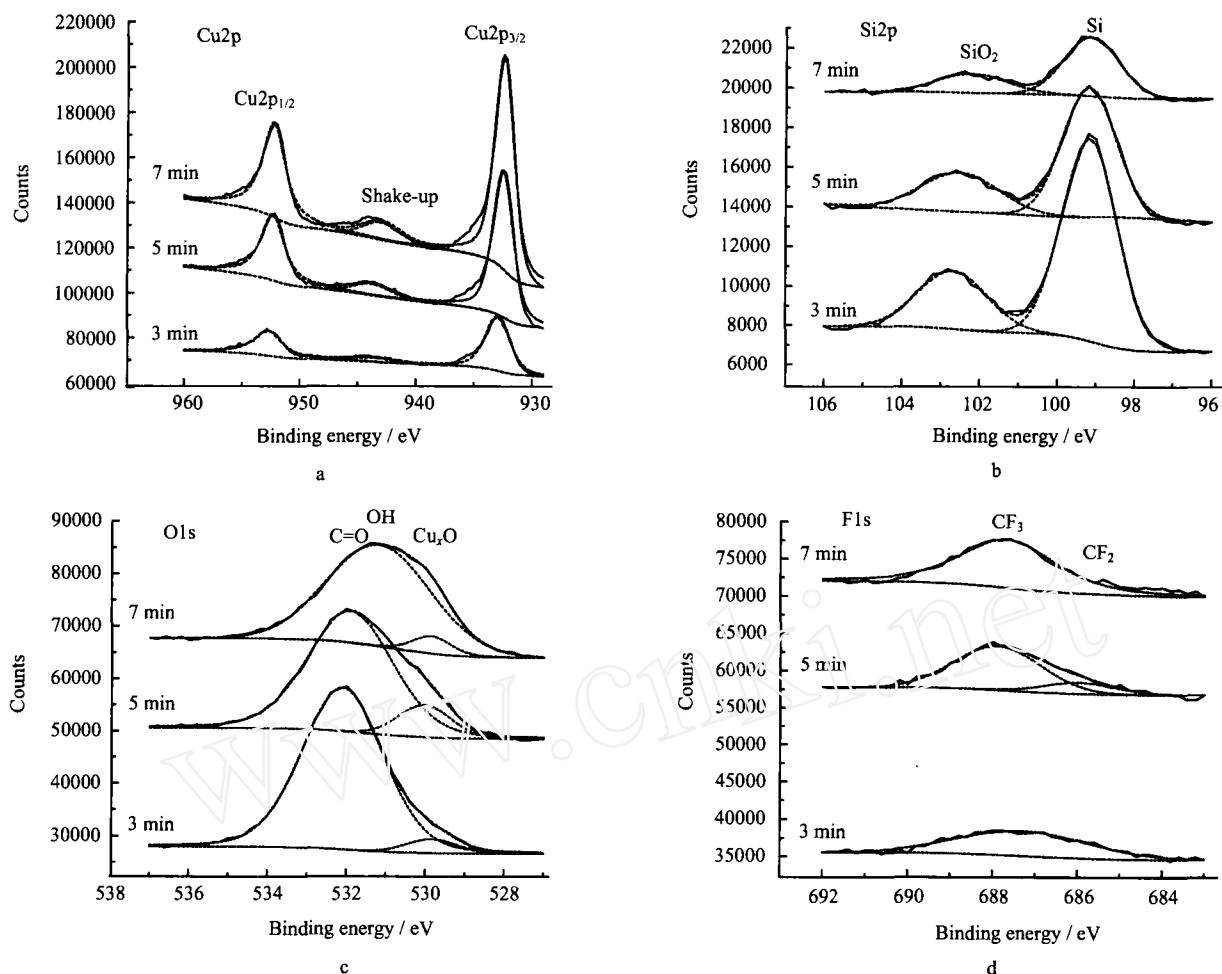


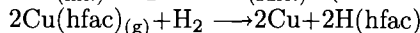
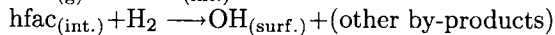
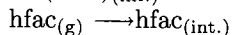
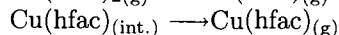
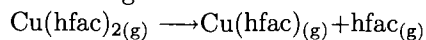
FIG. 5 XPS patterns of Cu films on Si substrate.

5300 ESCA [22], the C1s peak at 284.8 eV is attributed to the contaminated carbon, so C1s at 284.8 eV is used as the reference peak.

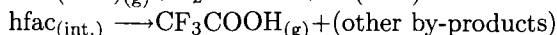
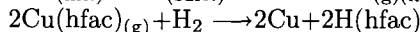
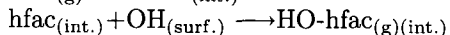
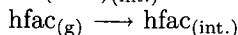
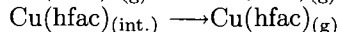
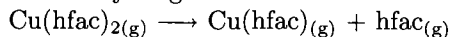
With the deposition processing, the intensity of the Si peaks in Si2p spectrum (Fig.5b) decreases and that of the Cu peaks in Cu2p spectrum (Fig.5a) increases, which indicates that the Si substrate is covered with Cu film. Figure 5c shows the high-resolution XPS spectra for O1s. The peak of O1s around 530.2 eV assigned to copper oxide appears from 3 to 7 min, which increases and then decreases. The major peak of O1s around 532.2 eV assigned to C=O decreases with the deposition time. After 7 min deposition, C=O almost disappeared whereas OH (531.5 eV) arises. It implies that the C=O is reduced to OH in H₂ atmosphere. As reported by Borgharkar [23], the CVD reaction can be enhanced by the OH group, which depends on its ability to dissociate the hydroxyl proton. Figure 5d shows the XPS spectra for F1s. The major peak of F1s around 687.5 eV assigned to carbon fluoride appears all the time, which illustrates that the hfac radical presents in the depo-

sition process. According to the mechanism of copper film deposited on SiO₂ substrate [24], and based on the XPS analysis, it can be concluded that the processing CVD copper film on Si substrate can be divided into two stages.

Initial stage:



Secondary stage:



where (g) and (int.) denote species in the form of gas and intermediate, respectively. (surf.) denotes that the group is presented on the surface.

At the initial stage, $\text{Cu}(\text{hfac})_2$ is thermally decomposed, and then H_2 reacts with hfac on the surface to produce OH. With the increasing deposition time, the reaction comes into secondary stage. When OH accumulates enough, it reacts with hfac, forming HO-hfac that desorbs, meanwhile, the copper oxide is reduced, and thus the redox reaction between $\text{Cu}(\text{hfac})_2$ and H_2 occurs.

IV. CONCLUSION

A versatile MOCVD system has been designed and constructed. Copper films were deposited on silicon(100) substrates by CVD using $\text{Cu}(\text{hfac})_2$ as a precursor. The growth mode of Cu nucleus is initially Volmer-Weber mode (island), and then transforms to Stranski-Rastanov mode (layer-by-layer plus island). From $\text{Cu}2p$, $\text{O}1s$, $\text{F}1s$, $\text{Si}2p$ patterns, the observed $\text{C}=\text{O}$, OH and CF_3/CF_2 should belong to $\text{Cu}(\text{hfac})_2$ formed by the thermal dissociation of $\text{Cu}(\text{hfac})_2$. H_2 reacts with hfac on the surface, producing OH. With its accumulation, OH reacts with hfac, forming HO-hfac, and desorbs, meanwhile, the copper oxide is reduced, and thus the redox reaction between $\text{Cu}(\text{hfac})_2$ and H_2 occurs.

V. ACKNOWLEDGMENT

This work was supported by the National Natural Science Foundation of China (No.20576112).

- [1] C. Y. Chang and S. M. Sze, *ULSI Technology*, New York: McGraw-Hill, 371 (1996).
- [2] S. Gandikota, S. Voss, R. Tao, A. Duboust, D. Cong, L. Y. Chen, S. Ramaswami and D. Carl, *Microelectr. Engng.* **50**(1-4), 501 (2000).
- [3] S. Kim, J. M. Park and D. J. Choi, *Thin Solid Films* **320**, 95 (1998).

- [4] D. Bollmann, R. Merke and A. Klumpp, *Microelectr. Engng.* **37/38**, 105 (1997).
- [5] S. Y. Chang, C. W. Lin, H. H. Hsu, J. H. Fang and S. J. Lin, *J. Electrochem. Soc.* **151**, C81 (2004).
- [6] H. H. Hsu, K. H. Lin, S. J. Lin and J. W. Yeh, *J. Electrochem. Soc.* **148**, C47 (2001).
- [7] T. O. Ogurtani and E. E. Oren, *J. Appl. Phys.* **96**, 7246 (2004).
- [8] S. P. Paul, *Nature* **406**, 1023 (2000).
- [9] T. L. Alford, *Thin Solid Film* **262**(1-2), vii (1995).
- [10] B. Zheng, G. Braeckelmann, K. Kujawski, I. Lou, S. Lane and A. E. Kaloyeros, *J. Electrochem. Soc.* **142**, 3896 (1995).
- [11] D. H. Kim, R. H. Wentorf and W. N. Gill, *J. Electrochem. Soc.* **140**, 3267 (1993).
- [12] S. Mukhopadhyay, K. Shalini, R. Lakshmi, A. Devi and S. A. Shivashankar, *Surf. Coat. Tech.* **150**, 205 (2002).
- [13] F. Shi, X. Ye, W. Yao and L. Cao, *Chin. J. Chem. Phys.* **11**(3), 261 (1998).
- [14] R. L. Puurunen, *Chem. Vap. Deposition* **10**, 159 (2004).
- [15] F. C. Frank and J. H. van der Merwe, *Proc. R. Soc. London Ser. A* **193**, 205 (1949).
- [16] M. Volmer and A. Z. Weber, *Phys. Chem.* **119**, 277 (1926).
- [17] I. N. Stranski and V. L. Krastanov, *Akad. Wiss. Lit. Mainz Math. Naturwiss Kl. Kar-August-Forest Lec.* **146**, 797 (1939).
- [18] C. Roland and G. H. Gilmer, *Phys. Rev. B* **47**, 16286 (1993).
- [19] J. A. T. Norman, D. A. Roberts, A. K. Hochberg, P. Smith, G. A. Petersen, J. E. Parmeter, C. A. Appleby and T. R. Omstead, *Thin Solid Films* **262**, 46 (1995).
- [20] S. Qi, J. Lv, Y. Zhang, S. Yang, Y. Wang and J. Wang, *Chin. J. Chem. Phys.* **14**, 459 (2001).
- [21] D. Ren, W. Wang, Y. Li and R. Yan, *Chin. J. Chem. Phys.* **17**, 87 (2004).
- [22] J. Q. Wang, *XPS/AES/UPS*, Beijing: National Defense Industry Press 519 (1992).
- [23] N. S. Borgharkar, G. L. Griffin, A. James and A. W. Maverick, *Thin Solid Films* **320**, 86 (1998).
- [24] K. Hanaoka, K. Tachibana, H. Ohnishi, *Thin Solid Films* **262**, 209 (1995).